View Article Online
View Journal

Faraday Discussions

Accepted Manuscript

This manuscript will be presented and discussed at a forthcoming Faraday Discussion meeting.
All delegates can contribute to the discussion which will be included in the final volume.

Register now to attend! Full details of all upcoming meetings: http://rsc.li/fd-upcoming-meetings

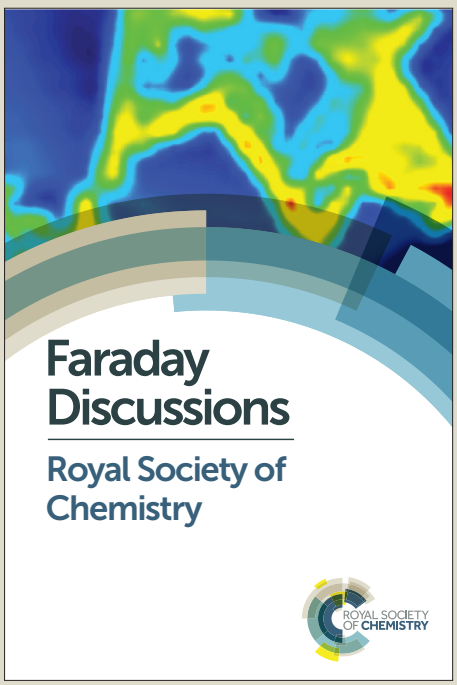

This is an *Accepted Manuscript*, which has been through the Royal Society of Chemistry peer review process and has been accepted for publication.

Accepted Manuscripts are published online shortly after acceptance, before technical editing, formatting and proof reading. Using this free service, authors can make their results available to the community, in citable form, before we publish the edited article. We will replace this *Accepted Manuscript* with the edited and formatted *Advance Article* as soon as it is available.

You can find more information about *Accepted Manuscripts* in the Information for Authors.

Please note that technical editing may introduce minor changes to the text and/or graphics, which may alter content. The journal's standard Terms & Conditions and the Ethical guidelines still apply. In no event shall the Royal Society of Chemistry be held responsible for any errors or omissions in this *Accepted Manuscript* or any consequences arising from the use of any information it contains.

This article can be cited before page numbers have been issued, to do this please use: A. Stikane, E. T. Hwang, E. V. Ainsworth, S. Piper, K. Critchley, J. Butt, E. reisner and L. J. C. Jeuken, *Faraday Discuss.*, 2018, DOI: 10.1039/C8FD00163D.

ROYAL SOCIETY OF CHEMISTRY

www.rsc.org/faraday_d

View Article Online
DOI: 10.1039/C8FD00163D

Towards Compartmentalized Photocatalysis: Multiheme Proteins as Transmembrane Molecular Electron Conduits

Authors: Anna Stikane[1,2], Ee Taek Hwang[1,2], Emma V. Ainsworth[3], Samuel Piper[3], Kevin Critchley[2,4], Julea N. Butt[*,3], Erwin Reisner[*,5], Lars J. C. Jeuken[*,1,2]

Affiliations:

1. School of Biomedical Sciences, University of Leeds, LS2 9JT, UK
2. The Astbury Centre for Structural Molecular Biology, University of Leeds, LS2 9JT, UK
3. Centre for Molecular and Structural Biochemistry, School of Chemistry and School of Biological Sciences, University of East Anglia, Norwich, NR4 7TJ, UK
4. School of Physics and Astronomy, University of Leeds, LS2 9JT, UK
5. Department of Chemistry, University of Cambridge, Cambridge, Lensfield Road, CB2 1EW, UK

Published on 21 December 2018. Downloaded by University of East Anglia Library on 1/2/2019 2:21:06 PM.

Faraday Discussions Accepted Manuscript

Abstract:

The high quantum efficiency of natural photosynthesis has inspired chemists for solar fuel synthesis. In photosynthesis, charge recombination in photosystems is minimized by efficient charge separation across the thylakoid membrane. Building on our previous bioelectrochemical studies of electron transfer between a light-harvesting nanoparticle (LHNP) and the decahaem subunit MtrC, we demonstrate photo-induced electron transfer through the full transmembrane MtrCAB complex in liposome membranes. Successful photoelectron transfer is demonstrated by the decomposition of a redox dye, Reactive Red 120 (RR120), encapsulated in MtrCAB proteoliposomes. Photoreduction rates are found to be dependent on the identity of the external LHNPs, specifically, dye-sensitized TiO_2, amorphous carbon dots (*a*-CD) and graphitic carbon dots with core nitrogen doping (*g*-N-CDs. Agglomeration or aggregation of TiO_2 NPs likely reduces the kinetics of RR120 reductive decomposition. In contrast, with the dispersed *a*-CD and *g*-N-CDs, kinetics of RR120 reductive decomposition is observed to be faster with MtrCAB proteoliposomes and we propose this is due to enhancement in the charge-separated state. Thus, we show a proof-of-concept for using MtrCAB as a lipid membrane-spanning building block for compartmentalised photocatalysis that mimics photosynthesis. Future work is focussed on incorporation of fuel generating redox catalysts in the MtrCAB proteoliposome lumen.

Introduction:

Global research efforts are continuously advancing strategies for harnessing solar energy into sustainable electricity, solar fuels and solar chemicals.[1–3] The light harvesting stage, *i.e.,* photo-induced charge separation and electron (or hole) transfer to electrode or catalyst, remains the principal efficiency-limiting step in these strategies.[3] In contrast, the stunning efficiency of biological light-harvesting systems results from a very precise and sophisticated arrangement of photosynthetic components: organic photosensitizers (*e.g.,* P680, P700, *etc.*), electron relay (chlorophyll, pheophytin, quinones, tyrosine *etc*.) and biocatalytic conversions (Q_B reduction/water splitting).[4] These components are optimized in the dimensions of space (relative location of components), energy (excited-state and redox properties) and time (rates of competing processes).[5,6] The composition of biological photosynthetic assemblies allows efficient photon absorption at light harvesting antennae, after which energy is passed along series of chromophores to the reaction centres (*e.g.,* plant photosystems I and II) , where is used for excitation of the P680/P700 cofactors.[4] Electrons ejected

View Article Online
DOI: 10.1039/C8FD00163D

from P680/P700 are relayed along an electron transfer chain and the light energy is ultimately stored as a transmembrane proton gradient and reduced redox-active molecules such as NADPH[7] (Figure 1a).

Such features as near-unity quantum yield and environmentally friendly operation put biological light-harvesting systems above any other known system with regard to initial steps of light harvesting for production of solar electricity and/or chemical synthesis.[7] Hence, there is a lot of interest in directly exploiting natural or genetically modified organisms[3,8–11] or their components for energy harvesting in artificial bio-hybrid systems.[12] Natural systems such as photosystem I, photosystem II and whole plant thylakoid membranes have been directly coupled to electrodes and inorganic catalysts in various photosynthetic devices to directly produce electricity, fuel (*e.g.,* molecular hydrogen) or evolve oxygen.[12–19] However, light-induced damage and degradation limits the use of pigment-protein complexes, especially photosystem II.[12,20] Alternative approaches are being developed where synthetic light-harvesting analogues are interfaced to (bio)catalyst to biomimic the general principles of natural photosynthesis.[6,7] Reported systems include examples in which photosensitizers (PSs) (*e.g.*, porphyrins) and light-harvesting nanoparticles (LHNPs) (*e.g.,* quantum dots) are interfaced with various conductive materials ranging from graphene to peptide nanotubes to semi-conductor nanoparticles, fuel producing enzymes and electron mediators to regenerate cofactors for redox enzymes.[7,21] Efforts are also made to explore the effects of photosynthetic component spatial organisation by mimicking such natural systems as stacked plant thylakoid membranes[22] and chlorosomes of green sulfur bacteria[23].

In this work, we aimed to mimic another aspect of plant photosynthesis, *i.e.,* the use of a lipid membrane to arrange and spatially separate photosynthetic components between the different environments of thylakoid lumen and stroma (Figure 1a).[4] Specifically, the objective was to spatially separate photo-oxidation and reduction reactions in the external and internal space of liposome compartments, respectively (Figure 1b). Thus, the envisioned system requires four components: 1) PSs or LHNPs to harvest light energy on the outside of liposomes, 2) transmembrane electron transfer, 3) reduction catalyst within the liposome compartment (lumen) to chemically store the light energy and 4) oxidation catalyst outside the liposome to regenerate the PS or LHNP.

We chose synthetic LHNPs over their natural equivalents (*e.g.,* plant photosystems I and II) because they are simpler and cheaper to produce and because of their stability and chemical inertness.[24–26] Three LHNPs were compared: dye-sensitised TiO_2 nanoparticles and two types of carbon dots. Dye-sensitized TiO_2 nanoparticles are well-studied and among most active photocatalyst materials.[24] We used TiO_2 nanoparticles photosensitized with a Ru(II)(bipyridine)$_3$ dye in which one of the bipyridines is phosphonated in the 4,4'-positions to enable chemisorption to TiO_2 (**RuP**-TiO_2, see Hwang et al. [27]). Carbon dots form another group of emerging light-absorbing nanomaterials showing remarkable photo-stability, water solubility, low toxicity and sustainable and cost-effective synthesis avoiding use of rare metals.[25,26,28] Here we test amorphous carbon dots (*a*-CD)[25] and graphitic carbon dots with core nitrogen doping (*g*-N-CDs).[28,29]

To transfer electrons across the lipid membrane after light harvesting, an icosa-heam transmembrane protein MtrCAB was employed (Figure 1c), which provides an electron-transfer relay through the otherwise insulating lipid membrane.[30,31] MtrCAB is a heterotrimeric protein (MtrA, MtrB, MtrC) found in the bacterium *Shewanella oneidensis* MR1, where it forms a 20 haem long conductive molecular 'wire' across the bacterial outer membrane.[30,31] This enables the bacterium to use insoluble minerals such as iron and manganese oxides as external electron acceptors for its anaerobic metabolism.[32] When incorporated to span the lipid bilayer of a proteoliposome, MtrCAB exhibits fast transmembrane electron transfer estimated to 10^3–10^4 electrons per second by spectroscopic

Published on 21 December 2018. Downloaded by University of East Anglia Library on 1/2/2019 2:21:06 PM.

Faraday Discussions Accepted Manuscript

View Article Online
DOI: 10.1039/C8FD00163D

reduction of encapsulated methyl viologen[33]. We have previously demonstrated efficient electron exchange between the soluble decahaem subunit MtrC and LHNPs.[34–36]

In the presented study, electrons are transferred via MtrCAB to the liposome lumen, where we envision they could generate fuel (such as hydrogen) by a fuel-generating catalyst. In this proof-of-concept study, electron transfer is optically monitored (539 nm) by a destructive reduction of an encapsulated azo dye, Reactive Red 120 (RR120, Figure S1).[37–39] RR120 contains two azo bonds (R–N=N–R'), each of which requires a transfer of four electrons in order to be cleaved to a colourless (pale yellow) product (Figure S1 c), *i.e.*, 8 electrons per RR120.[38] The optical signatures revealing heam redox status (Figure S2) are also monitored.

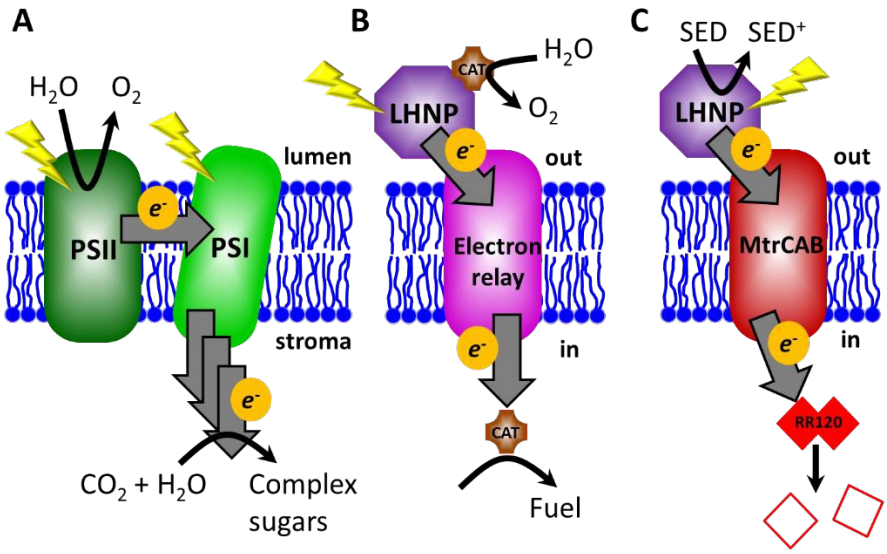

Figure 1 Schematic of light-driven electron transfer across the lipid membrane in nature (**a**), in the envisioned bio-mimicking system (**b**), and as presented in this study (**c**). (**a**) Photosystems I and II (PSI, PSII) are photo-excited and electrons are transferred via several electron acceptors across the membrane, where they are ultimately used for CO_2 conversion into complex sugars. (**b**) External electrons are supplied photo-chemically from a light-harvesting nanoparticle (LHNP), which is regenerated by a water-oxidising catalyst (CAT). Electrons are relayed across the membrane to a catalyst leading to fuel generation within the compartment. (**c**) Electron transfer across the lipid bilayer is ensured via transmembrane protein complex MtrCAB and monitored following reductive bleaching of an internalised red azo dye, Reactive Red 120 (RR120). SED – sacrificial electron donor

Materials and Methods:

Unless stated otherwise, all chemical substances were obtained from commercial suppliers and used without further purification: 3-(N -morpholino)propansulfonic acid (MOPS, >99.5%), sodium sulphate (Na_2SO_4, analytical reagent grade), N,N-Dimethyldodecylamine N-oxide (LDAO, BioXtra, >99%), sodium hydrosulfite (DT, >82%) and Reactive Red 120 azo dye (RR120) were purchased from Sigma–Aldrich. Ethylenediaminetetraacetic acid disodium salt dehydrate (EDTA, >99.5%) and *n*-octyl glucoside (OG, laboratory grade) were acquired from Melford and Triton X100 detergent (electrophoresis grade) was purchased from Fisher Chemicals. Milli-Q system was used to generate ultrapure water (resistance 18.2 MΩ·cm) which was used throughout. Ruthenium (Ru) dye sensitized TiO_2 anatase nanoparticles (**RuP**-TiO_2, diameter 6.8 ± 0.7 nm), *g*-N-CD (diameter 3.1 ± 1.1 nm) and *a*-CD (diameter 6.8 ± 2.3 nm) were synthesized an characterized as described previously.[25,27,29,40,41] *Shewanella oneidensis* MR1 protein MtrCAB was purified in Triton X-100 as described before.[42] The detergent exchange into 5 mM LDAO and additional purity resolution was performed using Superdex 200 Increase (GE Healthcare) eluted with 5mM LDAO, 20 mM HEPES pH 7.8. Purity of the purified

Published on 21 December 2018. Downloaded by University of East Anglia Library on 1/2/2019 2:21:06 PM.

Faraday Discussions Accepted Manuscript

View Article Online
DOI: 10.1039/C8FD00163D

MtrCAB was confirmed by SDS-PAGE with protein visualized by Coomassie and haem stain.[43] *Escherichia coli* polar lipid extracts were purchased from Avanti Polar Lipids and stored in 5 mg dry aliquots under nitrogen atmosphere at -20°C.

Preparation of MtrCAB proteoliposomes

5 mg *E. coli* polar lipid extract was dissolved by vigorous vortexing for up to 20 minutes in 294 µL MOPS buffer (20 mM MOPS, 30 mM Na_2SO_4, pH 7.4) containing 6.6 mM RR120 and 85 mM OG. 50.5 µL of 10 µM MtrCAB (or 5 mM LDAO for control liposomes) was added to the lipid solution and kept on ice for further 10 min. The sample was then rapidly diluted while mixing in 50 mL ice-cold 20 mM RR120 in MOPS buffer. The sample was transferred to an ultracentrifuge tube (polycarbonate) and centrifuged for 100 min at 71 000 g at 4 °C. The supernatant containing most of the non-encapsulated RR120 was discarded and the pellet was re-suspended in 500 µL MOPS buffer. The resulting sample was then centrifuged at 5000 g for about 5 min to pellet any aggregates. Remaining non-encapsulated RR120 was removed by two consecutive rounds of 60 min sample incubation with 0.6 g Bio-Beads (Bio-Rad SM-2) per 1 mL of sample at 4°C on a rolling shaker. Experiments were performed within 2 days of liposome preparation.

Liposome characterization

The concentration and size distribution of liposomes was determined by nanoparticle tracking analysis (NTA) using Nanosight (NS300, Malvern Panalytical). Liposome size was also determined by dynamic light scattering (DLS) using Zetasizer Nano Z (Malvern Panalytical). The size and volume of liposomes were estimated by treating liposomes as spherical particles with the average diameter based on NTA data.

The amount of reconstituted MtrCAB was determined using a BCA assay (ThermoFisher Scientific). As the absorbance of encapsulated RR120 overlaps with BCA reagent absorbance, liposomes were first lysed with 0.1 % v/v Triton X100 and RR120 was removed by two consecutive desalting columns (0.5 ml Zeba™ Spin, ThermoFisher) according to manufacturer's protocol. The effectiveness of the desalting columns was confirmed using a control sample of RR120 loaded liposomes without MtrCAB.

Reduction of RR120 encapsulated in MtrCAB proteoliposomes

Samples for photo-reduction experiments were assembled in a nitrogen atmosphere (glovebox, O_2 < 0.1 ppm) to ensure an anaerobic environment. MtrCAB proteoliposome samples were diluted 10-fold in MOPS buffer containing 50 mM sacrificial electron donor (EDTA). Appropriate amount of 10 mg/ml photosensitiser stock (27 µmol NP/L **RuP**-TiO_2, 476 µM *g*-N-CD or 44 µM *a*-CD; mass of particles is estimated based on size determined by EM and density of material) was added to 1 µmol LHNP/L final concentration. The cuvette was then sealed airtight and removed from glovebox for UV-vis absorbance spectroscopy (Cary 5000 UV-Vis-NIR, Agilent) fitted with an integrating sphere (Internal DRA-900, Agilent). UV-vis absorbance spectra were measured after 10 sec, 50 sec, 60 sec, 120 sec or in some cases 300 sec of sample irradiation using a cold light source holding a 150 W (15 V) halogen lamp (OSRAM) with a fibre optic arm (Krüss KL5125). The sample was placed 10 cm from the light source and irradiated. The light intensity at the sample under these conditions is approximately 450 ± 40 mW/cm^2 at 400 nm. Afterwards, the chemical reductant DT was added (final concentration 27 mM) to monitor further possible reduction of RR120. Finally, Triton X100 detergent was added (final concentration 0.045% v/v) to lyse the lipid vesicles and observe reduction of any remaining RR120. Control experiments testing reduction by DT (*i.e.,* without LHNP) were also performed. Photo-reduction control experiments with non-encapsulated RR120 were performed as above, but with 10 µM RR120, 50 mM EDTA and 1 µmol LHNP/L PS in MOPS buffer. The recovery yield of MtrCAB was

Published on 21 December 2018. Downloaded by University of East Anglia Library on 1/2/2019 2:21:06 PM.

Faraday Discussions Accepted Manuscript

observed to vary between proteoliposome preparations (see Results). To account for this, comparisons of encapsulated RR120 (photo)reduction by DT and photosensitisers were made based on proteoliposomes from the same preparation.

View Article Online
DOI: 10.1039/C8FD00163D

Treatment of UV-visible spectroscopy data

Spectroscopy data were corrected for sample dilution and for variation in background signal (by setting absorbance at 750 nm as the zero absorbance for each spectrum). Absorbance at 539 nm was selected to follow changes in RR120 absorbance over time, because it is less influenced by the absorbance of reduced MtrCAB (α- and β- haem peaks at 552 and 522 nm). In order to correct for the contribution of liposome scattering, the optical density outside the RR120 absorbance peaks was measured at 440 and 610 nm, *i.e.*, either side of the RR120 absorbance, and the average value was subtracted.

Results:

Characterization of MtrCAB liposomes

MtrCAB proteoliposomes loaded with the dye RR120 were prepared as described in the methods section. (Proteo)liposomes from each preparation were characterized to determine their size, concentration and amount of reconstituted MtrCAB and encapsulated RR120 as described in materials and methods. Although the size of MtrCAB proteoliposomes showed some batch-to-batch variation, proteoliposomes were consistently between 100 and 200 nm in diameter (Figure S3). The reconstitution protocol generated about 10^{13} liposomes/mL and thus an estimated total lumen volume in the order of 10-30 µL per mL of sample. Approximately 43 ± 13 % of initial MtrCAB was present in the reconstituted proteoliposomes with an estimated ratio of 10-50 MtrCAB proteins per liposome (depending on liposome size) assuming an even distribution across the liposomes.

Estimation of the amount of RR120 encapsulated in MtrCAB proteoliposomes was performed spectroscopically using optical absorbance at 534 nm ($\epsilon_{534\ nm}$ = 31.8 $mM^{-1}cm^{-1}$ was determined here using titration). It was estimated that, on average RR120 concentration in liposome lumen was ~10 mM, *i.e.*, the same order of magnitude as during liposome formation.

MtrCAB provides electron transfer across the bilayer

The ability of MtrCAB to transfer electrons across the membrane and reductively degrade RR120 was confirmed using an excess chemical reductant (DT; Figure 2). DT (E_m approximately -0.41 V vs SHE at pH 7.4)[44] reduced MtrCAB (haem potential window ranging from -0.45 to 0 V vs SHE)[45] within the time resolution of the experiment (< 20 s), as indicated by a shift of MtrCAB Soret peak due to haem absorbance (from 410 to 420 nm, Figure 2a). This is followed by a slower (minutes) decrease of RR120 absorbance (450-570 nm, RR120 becomes reductively bleached at ≤ -0.4 V vs SHE[46]), confirming the destructive reduction of the encapsulated RR120 (Figure 2a). Only ~10 % of RR120 was reduced in control experiments using liposomes without MtrCAB, indicating that RR120 is protected from reductive bleaching when inside liposomes and that reduction of encapsulated RR120 proceeds only if MtrCAB is present (Figure 2b). As a positive control, detergent (Triton X100, TX) was added at the end of the experiment to lyse the liposomes. This is followed by the immediate reductive bleaching of any remaining and now released RR120 (Figure 2a and b, green lines). The rates of reduction of encapsulated RR120 were observed to vary between MtrCAB proteoliposome preparations, likely due to the fact that MtrCAB recovery yields varied (see above). For this reason, (photo)reduction of encapsulated RR120 by different reductants (*i.e.,* DT, LHNPs) was compared using proteoliposomes from the same preparation. In such studies the relative rates of RR120 reduction by the different LHNPs are as reported by the representative data shown below.

Published on 21 December 2018. Downloaded by University of East Anglia Library on 1/2/2019 2:21:06 PM.

Faraday Discussions Accepted Manuscript

Published on 21 December 2018. Downloaded by University of East Anglia Library on 1/2/2019 2:21:06 PM.

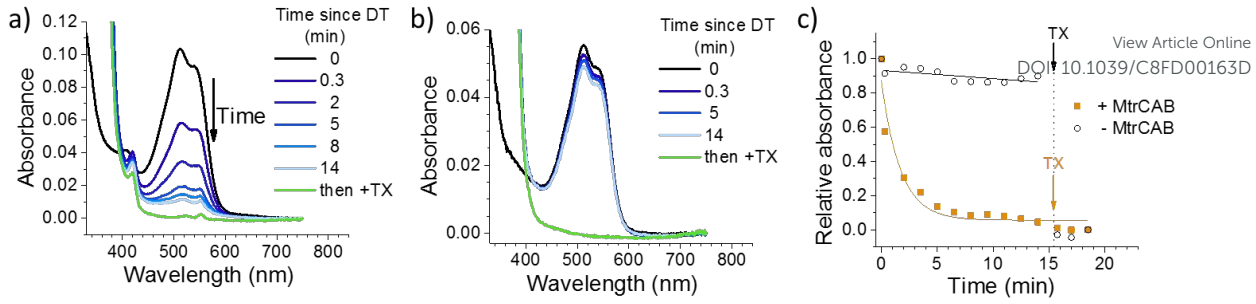

Figure 2 Chemical reduction of encapsulated RR120 by sodium dithionite (DT) with (**a**) and without (**b**) MtrCAB. Reduction is followed optically by monitoring absorbance of MtrCAB haems (oxidised peak at 410 nm, reduced peak at 420nm) and RR120 (oxidised 450-570 nm region). Black – oxidized sample; Blue – intact liposomes after addition of sodium dithionite; Green - sample after disruption of proteoliposome bilayer by detergent (Triton X100, TX). Time points indicate the time passed since the addition of DT. (**c**) Decrease of RR120 absorption (λ=539 nm) over time using liposomes with and without MtrCAB. Yellow and black lines show exponential and linear fits to the data, respectively.

Photoreduction across the membrane

Three different LHNPs, *i.e.,* **RuP** dye sensitized TiO_2 nanoparticles (**RuP**-TiO_2)[27], amorphous carbon dots (*a*-CD)[25] and graphitic carbon dots with core nitrogen doping (*g*-N-CDs)[28,29], were tested for photoreduction of RR120 encapsulated in liposomes with and without MtrCAB (Figure 3 a,b). All LHNPs have been previously shown to have sufficiently low reducing potential (< -0.45 V vs SHE)[29,47] to be able to reduce methyl viologen, and thus MtrCAB and RR120. Consistent with the data above, in the absence of MtrCAB, the majority (>70%) of RR120 was protected from photoreduction inside the liposome compartments (Figure 3a). However, subsequent addition of DT to all samples showed that slightly more RR120 was reduced in samples exposed to *g*-N-CD and **RuP**-TiO_2 compared to 'DT only' control (compare black open circles to blue data points in Figure 3a). This could suggest that small amounts of RR120 are released from liposomes due to interactions between **RuP**-TiO_2/*g*-N-CD and the liposomes. To further quantify this, well-established vesicle leakage assays were performed using a self-quenching dye, carboxyfluorescein[48]. No significant leakage was observed upon addition of any of the LHNPs, indicating no or very limited damage is incurred to the vesicles by the LHNPs.

In the presence of MtrCAB, all three LHNPs photo-reduced the encapsulated RR120 (Figure 3b). These experiments used 1 µM LHNPs, with an estimated ratio of 45 ± 2 LHNP per MtrCAB. **RuP**-TiO_2 and *g*-N-CD showed the fastest photoreduction, but with a rate lower compared to DT. Both *g*-N-CDs and *a*-CD showed a short 1–2 min delay from the start of irradiation till the onset of RR120 photoreduction. This delay is further referred as the 'lag phase' throughout this paper. The quantification of MtrCAB haem photoreduction by all three LHNPs was also attempted. Unfortunately, haem difference spectra could not be used due to spectral overlap with changes in RR120 and DT absorbance. Instead the first derivatives of all spectra was used instead as this is less sensitive to the background absorbance (Figure S2 and S4). This approach suggested that most MtrCAB is photoreduced by **RuP**-TiO_2 within the first minute of irradiation. In case of *g*-N-CDs and *a*-CD, it appeared that MtrCAB became reduced after several minutes, a time that coincides with the initial lag phase of RR120 reduction. After the lag phase, MtrCAB appeared to be fully reduced by *g*-N-CDs, whereas only partial MtrCAB photo-reduction seem to be observed by *a*-CDs. This suggest that with *a*-CD, photo-reduction of RR120 is in large part rate limited by the photo-reduction of MtrCAB.

Finally, photo-reduction of RR120 in the MtrCAB proteoliposomes was compared to the direct photo-reduction of non-encapsulated RR120 (Figure 3c). **RuP**-TiO_2 showed faster photoreduction compared to the MtrCAB proteoliposomes, clearing >90 % in less than 2 min, in line with conclusion

Faraday Discussions Accepted Manuscript

View Article Online
DOI: 10.1039/C8FD00163D

that reduction in proteoliposomes is rate limited by the interaction between RR120 and MtrCAB. In contrast, *g*-N-CDs and *a*-CDs took significantly longer to directly photo-reduce RR120 compared to MtrCAB proteoliposomes, *i.e.,* about 20 min for *g*-N-CDs and for *a*-CDs it took more than 40 min to reduce even 50 % of RR120. Both LHNPs also showed longer and more variable kinetics, with lag phases up to 5 min for *g*-N-CDs and 10-20 min for *a*-CDs. These variations in photo-reduction could reflect heterogeneity within carbon dots, as observed before.[49,50]

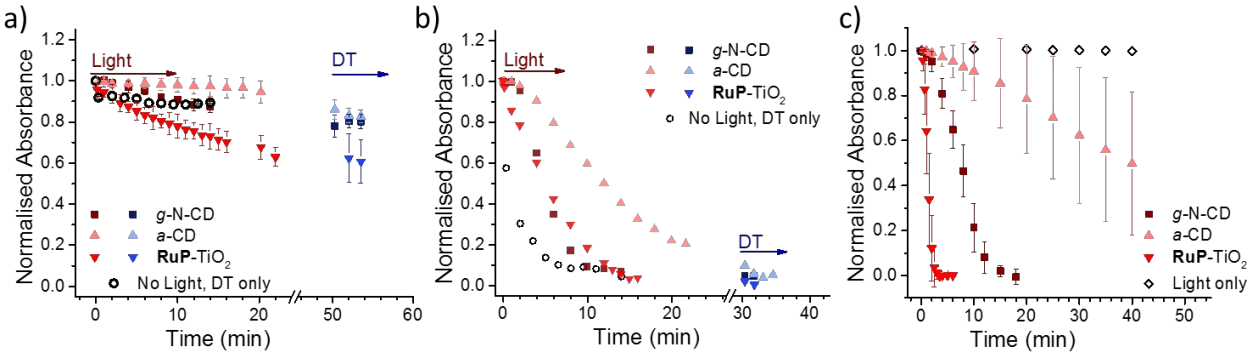

Figure 3 Photoreduction of RR120 encapsulated in liposomes without MtrCAB (**a**) and in MtrCAB proteoliposomes (**b**) followed by a decrease in the RR120 absorbance at 539 nm. Squares – *g*-NCD; Upward triangles – *a*-CD; Downward triangles – **RuP**-TiO_2 ; Red – sample after irradiation; Blue – sample after addition of DT; Black circles – chemical reduction using DT added at t=0 and without irradiation. Time points indicate cumulative time of irradiation. In case of DT, the time of DT addition is arbitrarily set to 50 and 30 min for (**a**) and (**b**), respectively, and following time points indicate time passed since addition of DT. (**c**) Direct photo-reduction of 10 µM RR120 in solution by LHNPs. White rhombus – irradiation of RR120 without LHNPs.

Discussion

In plant photosynthesis, a lipid membrane is used as a scaffolding to arrange and spatially separate photosynthetic components between the different environments of thylakoid lumen and stroma.[4] Here we mimic such physical separation and show a biomimetic photo-reduction across an insulating lipid membrane, where energy generated by external LHNPs is transferred across the lipid membrane via MtrCAB conduits to reduce electron acceptors located in the lumen of liposomes.

This system has several interfacial electron transfer steps: 1) LHNP to MtrCAB, 2) MtrCAB to RR120 and 3) SED to LHNP (Figure 1c). All experiments used excess amounts of SED (50 mM EDTA) and we have previously shown that the SED is not rate limiting for photo-reduction of MtrC by **RuP**-TiO_2.[27] As MtrCAB provided the electron relay across the membrane, the observed rate of RR120 reduction within liposomes will be dependent on the amount and distribution of MtrCAB within the liposome population. Chemical reduction of MtrCAB with DT was fast and instantaneous with respect to the time resolution of the experiments reported here. MtrCAB reduction by DT thus represent the fastest possible RR120 reduction within each liposome sample. The photoreduction by all three LHNPs was slower than reduction by DT, confirming that the overall rate of RR120 reduction was at least partly limited by the electron supply from LHNP to MtrCAB. However, for **RuP**-TiO_2 and *g*-N-CD, MtrCAB was almost fully reduced during the photo-reduction experiments, suggesting the reductive bleaching kinetics of RR120 were also rate limited by reduction of RR120 by MtrCAB. MtrCAB orientation in liposomes is not known and likely random, possibly further complicating the observed kinetics.

TiO_2 has high affinity for Glu/Asp protein residues[51–53], and **RuP**-TiO_2 has been shown before to bind strongly to MtrC and MtrCAB[36]. In addition, **RuP**-TiO_2 showed the best direct photo-reduction of non-encapsulated RR120. Despite this, photoreduction of RR120 in MtrCAB liposomes with **RuP**-TiO_2

Published on 21 December 2018. Downloaded by University of East Anglia Library on 1/2/2019 2:21:06 PM.

Faraday Discussions Accepted Manuscript

View Article Online
DOI: 10.1039/C8FD00163D

Published on 21 December 2018. Downloaded by University of East Anglia Library on 1/2/2019 2:21:06 PM.

was slower compared to chemical reduction with DT. We attribute the slower photoreduction of RR120 in MtrCAB proteoliposomes to the self-agglomeration or aggregation of **RuP**-TiO_2 particles, as observed with cryo-electron microscopy analysis (Figure S5). Hence, interaction between MtrCAB and **RuP**-TiO_2 might have been impaired. In contrast, the interaction between MtrCAB and both *g*-N-CDs and *a*-CDs is likely to be transient as no aggregation was detected upon mixing of the particles with MtrCAB liposomes. Nevertheless, for both carbon dots, relaying the electrons via MtrCAB improved bleaching rate of RR120 remarkably, which is up to four times faster in MtrCAB proteoliposomes compared to the direct photoreduction of RR120. Encapsulation of RR120 at mM concentration in the small lumen of the liposomes (compared to 10 µM RR120 in the control experiments with direct photoreduction) will enhance reduction kinetics by MtrCAB and, indeed, reduction of RR120 by MtrCAB was not observed to be rate limiting for α-CD. The enhanced photobleaching kinetics in the proteoliposome are thus due to a faster reduction of MtrCAB (at concentrations << 10 µM) compared to free RR120. We propose that this enhancement is due to the MtrCAB conduit, which can accumulate multiple electrons on its 20 haems, improving the rate of the multi-electron reduction required to bleach each RR120 molecule. In this respect, MtrCAB is able to stabilise the charge separated intermediate for the photo-reduction of RR120, mimicking the role of the chlorophyl/pheophytin/Q_A electron relay of the natural photosystems I and II.

These results provide an insight into how control over the nano-device organization and assembly can be used in artificial photosynthesis and solar-fuel catalyst design to enhance catalytic and quantum efficiencies. This work adds to the ongoing work in which the organisation of different photosynthetic components is exploited for (bio-)nanocatalysis.[7] For example, stacked multilayers of lipid membranes containing PSII[22] have been shown to increase production of ATP due to highly efficient exchange of substrates, while limiting diffusion of photo- and catalytic centres. Besides lipid membranes, various other template materials such as viruses, graphene and peptide fibres have been used to gain control over precise physical distribution of porphyrin PSs and catalytic reaction centres (*e.g.,* Pt, TiO_2 and IrO_2 clusters).[54–59] A 10-times higher yield for selective CO_2 conversion into methanol was reported using hollow graphene-doped nanofibers (G-fibers).[59] In this case, multiple enzymes required for methanol generation were confined within the nanofibers, and the photo-excited electrons were transported through the graphene fibers from photosensitizers located on the outside.[59] In a similar approach, photo-oxidation was separated from photo-reduction reactions by employing hierarchical cobalt oxide – silica core-shell nanotube arrays, where water oxidation and photo-reduction was confined to the inner and outer surface of nanotubes, respectively.[60] Many other ideas for building architectures with isolated environments for separated photo-oxidation and reduction can be drawn from the field of artificial nano-compartments, which has reported use of various materials ranging from labile biological liposomes, protein cages and virus capsids to rigid synthetic polymersomes and hybrid vesicles.[61–63]

Conclusion and future perspective

Here, we show a proof-of-concept of using the transmembrane MtrCAB conduit for compartmentalized photo-reduction. Three LHNPs demonstrated efficient photo-reduction of a liposome-encapsulated dye using MtrCAB as an electron relay. The rate with which two different carbon dots photo-reduced the encapsulated dye was improved in the liposome system. This example demonstrated how incorporation of a scaffolding material to separate photo-oxidation and reduction reactions can be beneficial for overall efficiency of solar energy harvest. In particular, we propose that MtrCAB can aid in the stabilisation of the charge separated state, improving quantum yield. Such

Faraday Discussions Accepted Manuscript

View Article Online
DOI: 10.1039/C8FD00163D

component could be beneficial to further advance artificial photosynthesis strategies and other (bio-)nanocatalysis applications. To further explore the potential use of MtrCAB conduit and nano-compartments, MtrCAB compartments should be tested for photosynthetic production of solar fuels or solar chemicals. In this case, a catalyst can be encapsulated in the liposomes, which enables a PS/LHNP to function in a separate environment from the fuel-generating catalyst. Finally, the lipids and/or MtrCAB could be replaced by synthetic components to explore other compartmentalised and structured molecular nano-architectures.

Conflicts of Interest

The authors declare no conflicts of interest.

Acknowledgements

This work was supported by the BBSRC (DTP studentship 1827308; grants BB/K009753/1, BB/K010220/1 and BB/K009885/1) the Engineering and Physical Sciences Research Council (PhD studentship 1307196). We thank Dr Manuela A. Gross for synthesizing **RuP**, Dr Daisuke Hojo for TiO_2 particles and Dr Benjamin C. M. Martindale for providing the carbon dot samples.

References

1 M. A. Green, *Nat. Energy*, 2016, **1**, 15015.

2 S. Ardo, D. Fernandez Rivas, M. A. Modestino, V. Schulze Greiving, F. F. Abdi, E. Alarcon Llado, V. Artero, K. Ayers, C. Battaglia, J.-P. Becker, D. Bederak, A. Berger, F. Buda, E. Chinello, B. Dam, V. Di Palma, T. Edvinsson, K. Fujii, H. Gardeniers, H. Geerlings, S. M. H. Hashemi, S. Haussener, F. Houle, J. Huskens, B. D. James, K. Konrad, A. Kudo, P. P. Kunturu, D. Lohse, B. Mei, E. L. Miller, G. F. Moore, J. Muller, K. L. Orchard, T. E. Rosser, F. H. Saadi, J.-W. Schüttauf, B. Seger, S. W. Sheehan, W. A. Smith, J. Spurgeon, M. H. Tang, R. van de Krol, P. C. K. Vesborg and P. Westerik, *Energy Environ. Sci.*, 2018, **11**, 2768–2783.

3 D. Lips, J. M. Schuurmans, F. Branco Dos Santos and K. J. Hellingwerf, *Energy Environ. Sci.*, 2018, **11**, 10–22.

4 N. Nelson and A. Ben-Shem, *Nat. Rev. Mol. Cell Biol.*, 2004, **5**, 971–982.

5 M. Şener, J. Strümpfer, J. Hsin, D. Chandler, S. Scheuring, C. N. Hunter and K. Schulten, *ChemPhysChem*, 2011, **12**, 518–531.

6 V. Balzani, A. Credi and M. Venturi, *ChemSusChem*, 2008, **1**, 26–58.

7 J. H. Kim, D. H. Nam and C. B. Park, *Curr. Opin. Biotechnol.*, 2014, **28**, 1–9.

8 W. Wei, P. Sun, Z. Li, K. Song, W. Su, B. Wang, Y. Liu and J. Zhao, *Sci. Adv.*, 2018, **4**, eaap9253.

9 M. K. Sarma, S. Kaushik and P. Goswami, *Biomass and Bioenergy*, 2016, **90**, 187–201.

10 L. M. Lassen, A. Z. Nielsen, B. Ziersen, T. Gnanasekaran, B. L. Møller and P. E. Jensen, *ACS Synth. Biol.*, 2014, **3**, 1–12.

11 D. J. Vinyard, J. Gimpel, G. M. Ananyev, S. P. Mayfield and G. C. Dismukes, *J. Am. Chem. Soc.*, 2014, **136**, 4048–4055.

12 E. Musazade, R. Voloshin, N. Brady, J. Mondal, S. Atashova, S. K. Zharmukhamedov, I. Huseynova, S. Ramakrishna, M. M. Najafpour, J.-R. Shen, B. D. Bruce and S. I. Allakhverdiev, *J. Photochem. Photobiol. C Photochem. Rev.*, 2018, **35**, 134–156.

Published on 21 December 2018. Downloaded by University of East Anglia Library on 1/2/2019 2:21:06 PM.

Faraday Discussions Accepted Manuscript

View Article Online
DOI: 10.1039/C8FD00163D

Published on 21 December 2018. Downloaded by University of East Anglia Library on 1/2/2019 2:21:06 PM.

13 M. Miyachi, S. Ikehira, D. Nishiori, Y. Yamanoi, M. Yamada, M. Iwai, T. Tomo, S. I. Allakhverdiev and H. Nishihara, *Langmuir*, 2017, **33**, 1351–1358.

14 F. Zhao, F. Conzuelo, V. Hartmann, H. Li, M. M. Nowaczyk, N. Plumeré, M. Rögner and W. Schuhmann, *J. Phys. Chem. B*, 2015, **119**, 13726–13731.

15 M. Miyachi, K. Okuzono, D. Nishiori, Y. Yamanoi, T. Tomo, M. Iwai, S. I. Allakhverdiev and H. Nishihara, *Chem. Lett.*, 2017, **46**, 1479–1481.

16 L. M. Utschig, N. M. Dimitrijevic, O. G. Poluektov, S. D. Chemerisov, K. L. Mulfort and D. M. Tiede, *J. Phys. Chem. Lett.*, 2011, **2**, 236–241.

17 S. C. Silver, J. Niklas, P. Du, O. G. Poluektov, D. M. Tiede and L. M. Utschig, *J. Am. Chem. Soc.*, 2013, **135**, 13246–13249.

18 T. Noji, H. Suzuki, T. Gotoh, M. Iwai, M. Ikeuchi, T. Tomo and T. Noguchi, *J. Phys. Chem. Lett.*, 2011, **2**, 2448–2452.

19 K. P. Sokol, W. E. Robinson, J. Warnan, N. Kornienko, M. M. Nowaczyk, A. Ruff, J. Z. Zhang and E. Reisner, *Nat. Energy*, 2018, **57**, 10595–10599.

20 F. Zhao, S. Hardt, V. Hartmann, H. Zhang, M. M. Nowaczyk, M. Rögner, N. Plumeré, W. Schuhmann and F. Conzuelo, *Nat. Commun.*, 2018, **9**, 1973.

21 S. H. Lee, D. S. Choi, S. K. Kuk and C. B. Park, *Angew. Chemie - Int. Ed.*, 2018, **57**, 7958–7985.

22 Y. Li, J. Fei, G. Li, H. Xie, Y. Yang, J. J. Li, Y. Xu, B. Sun, J. Xia, X. Fu and J. J. Li, *ACS Nano*, 2018, **12**, 1455–1461.

23 M. Wang, J. Chen, T. Lian and W. Zhan, *Langmuir*, 2016, **32**, 7326–7338.

24 S. H. Lee, J. H. Kim and C. B. Park, *Chem. - A Eur. J.*, 2013, **19**, 4392–4406.

25 B. C. M. Martindale, G. A. M. Hutton, C. A. Caputo and E. Reisner, *J. Am. Chem. Soc.*, 2015, **137**, 6018–6025.

26 Y. Wang and A. Hu, *J. Mater. Chem. C Mater. Opt. Electron. devices*, 2014, **2**, 6921–6939.

27 E. T. Hwang, K. Sheikh, K. L. Orchard, D. Hojo, V. Radu, C.-Y. Lee, E. Ainsworth, C. Lockwood, M. A. Gross, T. Adschiri, E. Reisner, J. N. Butt and L. J. C. Jeuken, *Adv. Funct. Mater.*, 2015, **25**, 2308–2315.

28 G. A. M. Hutton, B. C. M. Martindale and E. Reisner, *Chem. Soc. Rev.*, 2017, **46**, 6111–6123.

29 B. C. M. Martindale, G. A. M. Hutton, C. A. Caputo, S. Prantl, R. Godin, J. R. Durrant and E. Reisner, *Angew. Chemie Int. Ed.*, 2017, **56**, 6459–6463.

30 M. J. Edwards, G. F. White, C. W. Lockwood, M. C. Lawes, A. Martel, G. Harris, D. J. Scott, D. J. Richardson, J. N. Butt and T. A. Clarke, *J. Biol. Chem.*, 2018, **293**, 8103–8112.

31 M. Breuer, K. M. Rosso, J. Blumberger and J. N. Butt, *J. R. Soc. Interface*, 2015, **12**, 20141117.

32 J. K. Fredrickson, M. F. Romine, A. S. Beliaev, J. M. Auchtung, M. E. Driscoll, T. S. Gardner, K. H. Nealson, A. L. Osterman, G. Pinchuk, J. L. Reed, D. a Rodionov, J. L. M. Rodrigues, D. a Saffarini, M. H. Serres, A. M. Spormann, I. B. Zhulin and J. M. Tiedje, *Nat. Rev. Microbiol.*, 2008, **6**, 592–603.

33 G. F. White, Z. Shi, L. Shi, Z. Wang, A. C. Dohnalkova, M. J. Marshall, J. K. Fredrickson, J. M. Zachara, J. N. Butt, D. J. Richardson and T. A. Clarke, *Proc. Natl. Acad. Sci. U. S. A.*, 2013, **110**, 6346–6351.

Faraday Discussions Accepted Manuscript

View Article Online
DOI: 10.1039/C8FD00163D

34 C.-Y. Lee, B. Reuillard, K. Sokol, T. Laftsoglou, C. Lockwood, Sam Rowe, E. T. Hwang, J.-C. Fontecilla-Camps, L. J. C. Jeuken, J. Butt and E. Reisner, *Chem. Commun.*, 2016, **52**, 7390–7393.

35 B. Reuillard, K. H. Ly, P. Hildebrandt, L. J. C. Jeuken, J. N. Butt and E. Reisner, *J. Am. Chem. Soc.*, 2017, **139**, 3324–3327.

36 E. V. Ainsworth, C. W. J. Lockwood, G. F. White, E. T. Hwang, T. Sakai, M. A. Gross, D. J. Richardson, T. A. Clarke, L. J. C. Jeuken, E. Reisner and J. N. Butt, *ChemBioChem*, 2016, **17**, 2324–2333.

37 F. Zhang, A. Yediler, X. Liang and A. Kettrup, *J. Environ. Sci. Heal. Part A*, 2002, **37**, 707–713.

38 A. B. dos Santos, F. J. Cervantes and J. B. van Lier, *Bioresour. Technol.*, 2007, **98**, 2369–2385.

39 M. C. Costa, F. S. B. Mota, A. B. Dos Santos, G. L. F. Mendonça and R. F. do Nascimento, *Quim. Nova*, 2012, **35**, 482–486.

40 S. A. Trammell, J. A. Moss, J. C. Yang, B. M. Nakhle, C. A. Slate, F. Odobel, M. Sykora, B. W. Erickson and T. J. Meyer, *Inorg. Chem.*, 1999, **38**, 3665–3669.

41 C. X. Guo, D. Zhao, Q. Zhao, P. Wang and X. Lu, *Chem. Commun.*, 2014, **50**, 7318.

42 G. R. Heath, M. Li, I. L. Polignano, J. L. Richens, G. Catucci, P. O'Shea, S. J. Sadeghi, G. Gilardi, J. N. Butt and L. J. C. Jeuken, *Biomacromolecules*, 2016, **17**, 324–335.

43 P. E. Thomas, D. Ryan and W. Levin, *Anal. Biochem.*, 1976, **75**, 168–176.

44 S. G. Mayhew, *Eur. J. Biochem.*, 1978, **85**, 535–547.

45 R. S. Hartshorne, C. L. Reardon, D. Ross, J. Nuester, T. a Clarke, A. J. Gates, P. C. Mills, J. K. Fredrickson, J. M. Zachara, L. Shi, A. S. Beliaev, M. J. Marshall, M. Tien, S. Brantley, J. N. Butt and D. J. Richardson, *Proc. Natl. Acad. Sci.*, 2009, **106**, 22169–22174.

46 C. Guarantini, A. G. Fogg and M. V. B. Zanoni, in *Proceedings of the Symposium on Chemical and Biological Sensors and Analytical Electrochemical Methods*. Pennington: Electrochemical Society Inc., 1997, vol. 97, n. 19, pp. 467-476.

47 J. Willkomm, K. L. Orchard, A. Reynal, E. Pastor, J. R. Durrant and E. Reisner, *Chem. Soc. Rev.*, 2016, **45**, 9–23.

48 J. N. Weinstein, R. Blumenthal and R. D. Klausner, in *Methods Enzymology*, Academic Press, 1986, vol. 128, pp. 657–668.

49 Y. Zhou, P. Y. Liyanage, D. L. Geleroff, Z. Peng, K. J. Mintz, S. D. Hettiarachchi, R. R. Pandey, C. C. Chusuei, P. L. Blackwelder and R. M. Leblanc, *ChemPhysChem*, 2018, **19**, 2589–2597.

50 J. B. Essner, J. A. Kist, L. Polo-Parada and G. A. Baker, *Chem. Mater.*, 2018, **30**, 1878–1887.

51 E. Reisner, J. C. Fontecilla-Camps and F. a Armstrong, *Chem. Commun.*, 2009, 550–552.

52 E. Reisner, D. J. Powell, C. Cavazza, J. C. Fontecilla-Camps and F. A. Armstrong, *J. Am. Chem. Soc.*, 2009, **131**, 18457–18466.

53 Y. Kang, X. Li, Y. Tu, Q. Wang and H. Ågren, *J. Phys. Chem. C*, 2010, **114**, 14496–14502.

54 Y. S. Nam, T. Shin, H. Park, A. P. Magyar, K. Choi, G. Fantner, K. A. Nelson and A. M. Belcher, *J. Am. Chem. Soc.*, 2010, **132**, 1462–1463.

55 Y. S. Nam, A. P. Magyar, D. Lee, J. Kim, D. S. Yun, H. Park, T. S. Pollom, D. A. Weitz and A. M.

Published on 21 December 2018. Downloaded by University of East Anglia Library on 1/2/2019 2:21:06 PM.

Faraday Discussions Accepted Manuscript

Belcher, *Nat. Nanotechnol.*, 2010, **5**, 340–344.

56 K. Liu, R. Xing, Y. Li, Q. Zou, H. Möhwald and X. Yan, *Angew. Chemie Int. Ed.*, 2016, **55**, 12503–12507.

57 K. Liu, M. Abass, Q. Zou and X. Yan, *Green Energy Environ.*, 2017, **2**, 58–63.

58 J. H. Kim, M. Lee, J. S. Lee and C. B. Park, *Angew. Chemie Int. Ed.*, 2012, **51**, 517–520.

59 X. Ji, Y. Kang, Z. Su, P. Wang, G. Ma and S. Zhang, *ACS Sustain. Chem. Eng.*, 2018, **6**, 3060–3069.

60 W. Kim, B. A. McClure, E. Edri and H. Frei, *Chem. Soc. Rev.*, 2016, **45**, 3221–3243.

61 S. Schmidt, K. Castiglione and R. Kourist, *Chem. - A Eur. J.*, 2018, **24**, 1755–1768.

62 L. Klermund and K. Castiglione, *Bioprocess Biosyst. Eng.*, 2018, **41**, 1233–1246.

63 S. Khan, M. Li, S. P. Muench, L. J. C. Jeuken and P. A. Beales, *Chem. Commun.*, 2016, **52**, 11020–11023.

View Article Online
DOI: 10.1039/C8FD00163D

Published on 21 December 2018. Downloaded by University of East Anglia Library on 1/2/2019 2:21:06 PM.

Faraday Discussions Accepted Manuscript